www.sciencemag.org/content/347/6227/1260/suppl/DC1

Supplementary Materials for

Interleukin-3 amplifies acute inflammation and is a potential therapeutic target in sepsis

Georg F. Weber,* Benjamin G. Chousterman, Shun He, Ashley M. Fenn, Manfred Nairz, Atsushi Anzai, Thorsten Brenner, Florian Uhle, Yoshiko Iwamoto, Clinton S. Robbins, Lorette Noiret, Sarah L. Maier, Tina Zönnchen, Nuh N. Rahbari, Sebastian Schölch, Anne Klotzsche-von Ameln, Triantafyllos Chavakis, Jürgen Weitz, Stefan Hofer, Markus A. Weigand, Matthias Nahrendorf, Ralph Weissleder, Filip K. Swirski*

*Corresponding author. E-mail: fswirski@mgh.harvard.edu (F.K.S.); georg.weber@uniklinikum-dresden.de (G.F.W.)

Published 13 March 2015, *Science* **347**, 1260 (2015)
DOI: 10.1126/science.aaa4268

This PDF file includes:

Materials and Methods

Humans

Human data from prospective measurements of Interleukin-3 and secondary analyses of patients participating in the RAMMSES-trial (German Clinical Trials Register: DRKS00000505). This observational clinical study was first approved by the local ethics committee (Trial-Code-Nr.: S123-2009) on June, 8th 2009. For the presented IL-3 measurements an amendment was submitted to the local ethics committee which was approved on November, 22th 2013. *Human data from prospective measurements of Interleukin-3 and analyses of patients participating in the SEPIL-3-trial.* This observational clinical study was first approved by the local ethics committee (Trial-Code-Nr.: EK 308082013) on September, 19th 2013. The observational clinical studies were conducted in the surgical intensive care unit of the University Hospital of Heidelberg, Germany, and the surgical intensive care unit of the University Hospital of Dresden, Germany. Study patients or their legal designees signed written informed consent. In total, 60 patients within the *RAMMSES-cohort* and 40 patients within the *SEPIL-3-cohort* with septic shock, classified according to the criteria of the International Sepsis Definitions Conference *(34)*, were enrolled with an onset of sepsis syndrome ≤ 24 hours. 3 patients in *SEPIL-3* were excluded from analysis for not meeting study criteria. Blood samples from patients were collected at sepsis onset, and 1, 4, 7, 14, and 28 days later. After blood collection, plasma of all study participants was immediately obtained by centrifugation, transferred into cryotubes, and stored at -80°C until further processing. Quantification of IL-3 in human plasma samples was performed using an enzyme linked immunosorbent assay kit (R&D Systems, Minneapolis, USA) in combination with chemiluminescent detection for increased sensitivity. The assays were performed according to the manufacturer's instructions and measured in a microplate reader set to luminescence mode (BMG Labtech, Ortenberg, Germany) with an integration time of 2 seconds per well, yielding a sensitivity of 3.9 pg/ml IL-3. Quantification of IL-1β, IL-6, and TNF-α in human samples was performed using an enzyme linked immunosorbent assay kit (R&D Systems, Minneapolis, USA) according to the manufacturer's

instructions. In the *SEPIL-3-trial* heparinized blood samples were immediately processed for flow cytometric analysis of leukocyte surface markers after Erythrocytes were lysed using RBC Lysis Buffer (BioLegend). *Spleen tissue (6 patients)*: After splenectomy for various indications (within an additional clinical study approved by the local ethics committee with Trial-Code-Nr.: EK 76032013; study patients signed written informed consent) fresh spleen samples were obtained, directly embedded in O.C.T. compound (Sakura), frozen at -80ºC, and stored for immunofluorescence staining and microscopy. Two additional spleens were directly processed for flow cytometric analysis. Spleen tissue was homogenized through a 40 µm-nylon mesh, after which erythrocyte lysis was performed on the spleen sample using RBC Lysis Buffer (BioLegend). Controls: Within the *RAMMSES*- and *SEPIL-3-trial* healthy volunteers without signs of sepsis served as controls.

Animals

Balb/c mice (WT), C57BL/6 (WT), and CByJ.B6-Tg(UBC-GFP)30Scha/J (GFP^+) female mice (from Jackson Laboratories) were used in this study. IL-3 deficient mice ($Il3^{-/-}$) on a Balb/c background were obtained from RIKEN BRC Laboratories, Japan. GM-CSF-deficient mice ($Csf2^{-/-}$) on a C57BL/6 background were bred in-house. All mice were 8-12 weeks of age at the time of sacrifice. All protocols were approved by the Animal Review Committee at Massachusetts General Hospital.

Animal models and *in vivo* interventions

Endotoxin-induced peritonitis and peritoneal lavage: Where indicated, mice were administered 25 µg of LPS (Sigma), by i.p. injections in PBS. *Cecal ligation and puncture (CLP):* This rodent model of sepsis was carried out as previously described *(9)*. In brief, the peritoneal cavity was opened during isoflurane anesthesia, and the cecum was exteriorized and ligated at different points distal of the ileo-cecal valve using a non-absorbable 7-0 suture. To induce high-grade CLP ~60-80% of the cecum was ligated; to induce mid-grade CLP ~30-50% of the cecum was ligated. The distal end of the cecum

was then perforated using a 23 G needle, and a small drop of feces was extruded through the puncture. The cecum was relocated into the peritoneal cavity and the peritoneum was closed. Animals were resuscitated by s.c. injection of 1 mL of saline. Age-matched controls were included for all procedures. In general, only experiments testing survival utilized high-grade CLP. *Splenectomy*: Under isofluorane anesthesia, the peritoneal cavity of mice was opened and the splenic vessels were ligated using a 6.0 silk suture. The spleen was then carefully removed. For control experiments, the peritoneum was opened, but the spleen was not excised. *Cell and protein transfer:* B1 cells, B1a cells, and GMP were FACS sorted from the peritoneum or bone marrow of WT, *Il3*$^{-/-}$, or naïve GFP^{+} mice. Cells were injected into the peritoneum or the tail vein of recipient mice as indicated. *IL-3 injection*: *Il3*$^{-/-}$ mice were injected with 5 µg recombinant IL-3 (R&D Systems), twice, in 50 µl PBS or 50 µl PBS alone into the tail vein 30 min and 12 h after CLP. WT animals were injected with an IL-3 complex, as previously described *(35)*. IL-3 (10 µg; R&D Systems) was mixed with anti-IL-3 Ab (5 µg; MP2–8F8, BD Pharmingen) at RT for 1 min and the complex (in 200 µl saline) was injected into each mouse into the tail vein at the beginning of the experiment. Mice were sacrificed at 24 h. *Anti-CD123 injection*: 200 µg anti-CD123 or 200 µg IgG1 isotype control (Biolegend) in 200 µl PBS were injected into the tail vein of WT mice 1, 6, and 24 h after CLP was performed. Mice were sacrificed at 24 h (cytokine analysis) or 48 h (cell analysis). *Phagocyte depletion*: To deplete neutrophils and monocytes, 200 µg of anti-Ly6G (isotype 1A8, Biolegend) antibody were injected into the tail vein 48 h before the CLP and 200 µl of clodronate liposome were injected into the tail vein 24 h and 6 h before CLP; control mice were injected with 200 µg IgG2a isotope control (Biolegend) and 200 µl of PBS liposomes. Mice were sacrificed at 24 h after CLP. Clodronate and PBS liposomes were obtained from clodronateliposomes.com. *Temperature:* The temperature of each animal was measured by rectal insertion of a temperature sensor while the mouse was under anesthesia. *Clinical score:* The clinical score of each animal was assessed as follows (points). [a] appearance: normal (0), lack of grooming (1), piloerection (2), hunched up (3), above and eyes half closed (4); [b] behaviour - unprovoked: normal (0), minor

changes (1), less mobil and isolated (2), restless or very still (3); behaviour - provoked: responsive and alert (0), unresponsive and not alert (3); [c] clinical signs: normal respiratory rate (0), slight changes (1), decreased rate with abdominal breathing (2), marked abdominal breathing and cyanosis (3); [d] hydration status: normal (0), dehydrated (5). The higher the score the worse the clinical situation of the animal. *Blood pressure measurement:* The blood pressure of WT and *Il3*$^{-/-}$ mice was measured by using a tail-cuff plethysmograph according to the manufacturer's instructions. Mice were placed on a 37ºC heated plate and measurements were performed 5 times/each animal. Per animal the mean systolic value was then calculated.

Cells

Isolation and ex vivo methods: Peripheral blood for flow cytometric analysis was collected by aortic puncture, using heparin as the anticoagulant. Erythrocytes were lysed using RBC Lysis Buffer (BioLegend). Total white blood cell count was determined by preparing a 1:10 dilution of (undiluted) peripheral blood obtained from the orbital sinus using heparin-coated capillary tubes in RBC Lysis Buffer (BioLegend). After organ harvest, single cell suspensions were obtained as follows: for bone marrow, the femur and tibia of one leg were flushed with PBS through a 40 µm-nylon mesh. The peritoneal space was lavaged with 3 × 3 ml of PBS to retrieve infiltrated and resident leukocytes. Spleens were homogenized through a 40 µm-nylon mesh, after which erythrocyte lysis was performed on the spleens using RBC Lysis Buffer (BioLegend). Liver, lung, thymus, lymph node tissue were cut into small pieces and subjected to enzymatic digestion with 450 U/ml collagenase I, 125 U/ml collagenase XI, 60 U/ml DNase I and 60 U/ml hyaluronidase (Sigma-Aldrich, St. Louis, MO) for 1 h at 37°C while shaking at 750 rpm. Total viable cell numbers were obtained using Trypan Blue (Cellgro, Mediatech, Inc, VA). To determine total bone marrow cellularity, one femur and one tibia were estimated to represent 7% of total marrow*(36)*. *In vitro:* For all *in vitro* experiments, cells were cultured in medium (RPMI-1640 medium supplemented with 5% fetal bovine serum, 25 mM HEPES, 2mM L- glutamine, 100 U/ml penicillin, and 100 U/ml streptomycin) or B

cell medium (medium + 50µM ß-mercaptoethanol), and kept in a humidified 5% CO_2 incubator at 37°C. For *in vitro* experiments involving IL-3 stimulation, bone marrow cells were stained with anti-Lineage-PE antibodies, followed by incubation with anti-PE MicroBeads (Miltenyi). Lin^- bone marrow cells were then negatively selected through MACS cell separation columns and separators (Miltenyi) for *in vitro* stimulation. Cells were seeded at a density of 50,000 cells/100µl in 24-well flat-bottom, or 96-well round-bottom plates (Corning) and cultured 24 or 96 h in medium. Where indicated, LPS was added at 1 µg/ml and rIL-3 was added at 20 ng/ml in PBS. To determine IgM production, serosal B1a cells were obtained from Balb/C (WT), C57BL/6 (WT), *Csf2*$^{-/-}$ and *Il3*$^{-/-}$ mice. Cells were sorted on a BD FACSAria II (BD Biosciences) and cultured at 37°C for 48h in B cell medium. Where indicated, LPS (Sigma) was added at a dose of 10 µg/mL.

Flow Cytometry

The following antibodies were used for flow cytometric analyses. *Mouse*: anti-CD43-FITC, S7 (BD Biosciences); anti-Ly6C-FITC, AL-21 (BD Biosciences); anti-Ly6G-FITC, 1A8 (BD Biosciences); anti-CD11b-FITC, M1/70 (BD Biosciences); anti-CD3e-FITC, 145-2C11 (BD Biosciences); anti-CD4-FITC, RM4-5 (BD Biosciences); anti-CD8-FITC, 53-6.7 (BD Biosciences); anti-IL-6-FITC, MP5-20F3 (BD Biosciences); anti-B220-PE, RA3-6B2 (BD Biosciences); anti-CD19-PE, 1D3 (BD Biosciences); anti-CD49b-PE, DX5 (BD Biosciences); anti-90.2-PE, 53-2.1 (BD Biosciences); anti-Ly6G-PE, 1A8 (BD Biosciences); anti-Ter119-PE, TER-119 (BD Biosciences); anti-IL-3-PE, MP2-8F8 (BD Biosciences); anti-GM-CSF-PE, MP1-22E9 (BD Biosciences); anti-CD131-PE, JORO50 (BD Biosciences); anti-CD123-PE, 5B11 (BioLegend); anti-IgG2A-PE, RTK2758 (BD Biosciences); anti-IgG1-PE, A85-1 (BD Biosciences); anti-CD11b-PE, M1/70 (BD Biosciences); anti-CD11c-PE, N418 (eBioscience); anti-CD127-PE, A7R34 (eBioscience); anti-CD11c-PerCPCy5.5, HL3 (BD Biosciences); anti-Ly6C-PerCPCy5.5, HK1.4 (eBioscience); anti-CD90.2-PECy7, 53-2.1 (BD Biosciences); anti-F4/80-PECy7, BM8 (BioLegend); anti-TLR4-PECy7, MTS510 (BioLegend); anti-ckit-PECy7, 2B8 (BD Biosciences); anti-Sca-1-PECy7, D7 (eBioscience); anti-CD45.2-

PECy7, 104 (BioLegend); anti-CD23-PECy7, B3B4 (BioLegend); anti-IL-1β, APC, NJTEN3 (eBioscience); anti-TNF-α-APC, MP6-XT22 (Bd Biosciences); anti-FceR1-APC, MAR-1 (eBioscience); anti-ckit-APC, 2B8 (BD Biosciences); anti-Annexin V-APC, anti-CD115-APC, AFS98 (eBioscience); anti-IgM-APC, II/41 (BD Biosciences); anti-CD8-APC, 53-6.7 (BD Biosciences); anti-CD19-biotin, 6D5 (BioLegend); anti-CD138-biotin, 281-2 (BD Biosciences); anti-CD123-biotin, 5B11 (BioLegend); anti-CD45.2-biotin, 104 (BioLegend); anti-Sca-1-Alexa Fluor 700, D7 (eBioscience); anti-MHCII-Alexa Fluor 700, M5/114.15.2 (eBioscience); anti-CD4-Alexa Fluor 700, GK1.5 (eBioscience); anti-CD19-APCCy7, 6D5 (BioLegend); anti-CD11b-APCCy7, M1/70 (BD Biosciences); anti-IgM-APCCy7, RMM-1 (BioLegend); anti-CD16/32-APCCy7, 2.4G2 (BD Biosciences); anti-CD4-Pacific blue, GK1.5 (BioLegend); anti-CD8-Pacific blue, 53-6.7 (BioLegend); anti-IgD-Pacific blue, 11-26c.2a (BioLegend); anti-CD45.2-Pacific blue (BD Biosciences); anti-CD19-Brilliant Violet 421, 6D5 (BioLegend); anti-IgM-Brilliant Violet 421, RMM-1 (BioLegend); anti-CD11b-Brilliant Violet 421, M1/70 (BioLegend). *Human*: anti-CD19-FITC, HIB19 (BD Biosciences); anti-CD16-FITC, 3G8 (BD Biosciences); anti-IL-3-PE, BVD3-1F9 (BD Biosciences); anti-IgG1-PE, R3-34 (BD Biosciences); anti-CD2-PE, RPA-2.10 (BD Biosciences); anti-CD3-PE, HIT3a (BD Biosciences); anti-CD15-PE, W6D3 (BD Biosciences); anti-CD19-PE, HIB19 (BD Biosciences); anti-CD20-PE, 2H7 (BD Biosciences); anti-CD56-PE, B159 (BD Biosciences); anti-NKp46-PE, 9-E2 (BD Biosciences); anti-HLADR-PerCP-Cy5.5, G46-6 (BD Biosciences); anti-CD20-PECy7, 2H7 (BD Biosciences); anti-CD14-PECy7, M5E2 (BD Biosciences); anti-IgM-APC, G20-127 (BD Biosciences); anti-CD123-APC, 7G3 (BD Biosciences); anti-CD45-Alexa Fluor 700, HI30 (BioLegend); anti-CD11b-APCCy7, ICRF44 (BD Biosciences); anti-CD3-BV421, UCHT1 (BioLegend); anti-CD11c-BV421, 3.9 (BioLegend). *Staining Strategies*: Streptavidin-Alexa Fluor 700, Streptavidin-Pacific blue or Streptavidin-Pacific orange (Invitrogen) were used to label biotinylated antibodies. Staining for intracellular cytokines was performed using BD Cytofix/Cytoperm Plus Kit (BD Biosciences) according to the manufacturer's instructions. Intracytoplasmatic IgM staining was done as previously described *(19)*.

Briefly, cells were stained for 30 min with a primary IgM antibody (Percp.Cy5.5 channel) in a high concentration (1:200) to ensure saturation of surface IgM together with additional surface antibodies in normal concentration (1:700). After cell membrane permeabilization using Cytofix/Cytoperm Plus Kit (BD Biosciences) intracytoplasmatic IgM was performed using the secondary IgM antibody (APC channel) in a lower concentration (1:350). Cells were defined as: (i) Monocytes ($Ly6C^{high/low}CD115^{+}CD11b^{+}MHCII^{-}CD11c^{-}F4/80^{low/int}Lin_1^{-}$ (mouse) or $CD16^{high/low}CD14^{high/low}CD11b^{+}CD11c^{-}Lin_1^{-}$ (human), (ii) neutrophils ($Ly\text{-}6C^{int}CD11b^{+}MHCII^{-}CD11c^{-}Lin_1^{+}$), (iii) macrophages ($F4/80^{+}MHCII^{+}CD11b^{int}CD90.2^{-}CD19^{-}$), (iv) T cells ($CD3^{+}CD4/8^{+}B220^{-}MHCII^{-}$), (v) HSPC ($ckit^{+}Lin_2^{-}$), (vi) HSC ($ckit^{+}Sca\text{-}1^{+}Lin_2^{-}$), (vii) CMP ($ckit^{+}Sca\text{-}1^{-}CD34^{+}CD16/32^{low}Lin_2^{-}$), (viii) MEP ($ckit^{+}Sca\text{-}1^{-}CD34^{-}CD16/32^{-}Lin_2^{-}$), (ix) GMP ($ckit^{+}Sca\text{-}1^{-}CD34^{+}CD16/32^{high}CD115^{-}Lin_2^{-}$), (x) MDP ($ckit^{+}Sca\text{-}1^{-}CD34^{+}CD16/32^{high}CD115^{+}Lin_2^{-}$), (xi) basophils ($CD49b^{+}FceR1^{+}ckit^{-}Lin_3^{-}$), (xii) mast cells ($FceR1^{+}ckit^{+}Lin_3^{-}$) (xiii) Serosal B1a cells ($CD45^{+}CD19^{+}IgM^{+}CD5^{+}CD43^{+}$), (xiv) Peritoneal macrophages ($CD45^{+}CD11b^{+}F4/80^{high}$). Lineages were defined as: Lin_1: Ly6G, B220, CD19, CD49b, Ter119, CD90.2 (mouse) or CD2, CD3, CD15, CD19, CD20, CD56, NKp46 (human); Lin_2: B220, CD19, CD49b, Ter119, CD90.2, CD11b, CD11c, IL-7R, Gr-1; Lin_3: B220, CD19, Ter119, CD3, CD4, CD8, Gr1. Data were acquired on an LSRII (BD Biosciences) and analyzed with FlowJo v8.8.6 (Tree Star, Inc.). Cells were sorted on a BD FACSAria II (BD Biosciences).

Histology

Mouse: The lungs, livers and spleens from Balb/c control mice and $Il3^{-/-}$ mice were harvested in steady state or 1 day after CLP and embedded in a 2-methylbutane bath (Sigma-Aldrich) on dry ice. The lungs were filled with a mixture of O.C.T. compound and PBS (1:1) through the tracheas prior to harvesting. Serial 6 µm thick fresh-frozen sections were prepared and stained with hematoxylin and eosin (H&E) for overall histological analysis. For immunohistochemical staining, the sections were incubated with anti-CD115 (AF598, eBioscience) and anti-Ly-6G (1A8, BioLegend), followed by a

biotinylated secondary antibody (Vector Laboratories, Inc.), and developed with 3-amino-9-ethylcarbazole (AEC, Dako). All sections were counterstained with hematoxylin and coverslipped using an aqueous mounting medium. The images were captured using a digital slide scanner, NanoZoomer 2.0RS (Hamamatsu). For immunofluorescence staining, spleen sections were incubated with anti-IL-3 biotin (MP2-8F8, BioLegend), anti-IgM-FITC (II/41, BD Biosciences), anti-CD11b-FITC (M1/70, BD Biosciences), anti-CD19-FITC (1D3, BD Biosciences), anti-CD3e-FITC (145-2C11, BD Biosciences), anti-CD117-FITC (c-kit 2B8, BD Biosciences), anti-CD90.2-Alexa Four 488 (30-H12, BioLegend), anti-CD49b-Alexa Fluor (HMα2, BioLegend), anti-CD11b-APC (M1/70, BD Biosciences). A biotinylated secondary antibody (Vector Laboratories, Inc.) and streptavidin-Alexa Fluor 594 (Invitrogen) were used to detect IL-3 positive cells. The slides were coverslipped using a mounting medium with DAPI (Vector Laboratories, Inc.) to identify the nuclei. Images were captured using a motorized fluorescence microscope, BX63 (Olympus). *Human*: IL-3 positive B-cells were visualized on frozen sections by immunofluorescence staining. Briefly, human spleen sections were embedded in O.C.T. compound and serial fresh- frozen sections (6 µm) were prepared. The sections were fixed with ice cold acetone for 10 min at -20°C. After washing (PBS with 5% BSA and 0.2% Triton X-100) sections were blocked with 0.3% goat serum (in washing buffer) for 30 min at room temperature. Thereafter, spleen sections were incubated with anti-IgM-FITC (G20-127, BD Pharmingen, 1/50), anti-CD19-FITC (HIB19, BD Pharmingen, 1/50), anti-IL-3-PE (BVD3-1F9, BD Pharmingen, 1/25), or IgG1-PE isotype control (1/25) (R3-34, BD Pharmingen, 1/25) overnight at 4°C. After washing, counterstaining was performed with DAPI and slides were coverslipped (10min at RT). After mounting, spleen sections were imaged with Axiovert 200 Inverted Fluorescence Microscope and Axiovision image processing software (Zeiss, Germany). The enumeration of IL-3 producing IgM^+ B cells in human spleens was conducted by blinded analysis of 6 field-of-views at 20× magnification. The average amount of IL-3 producing IgM^+ B cells per field-of-view is presented.

Molecular Biology

RT-PCR: Total RNA was isolated from whole tissue using the RNeasy Mini Kit according to the manufacturer's instructions. cDNA was generated from 1 µg of total RNA per sample using the High Capacity cDNA Reverse Transcription Kit (Applied Biosystems). Real time PCR was performed in triplicates using the TaqMan Gene Expression Assay System on a 7300 Real-Time PCR System (Applied Biosystems). Primers for IL-3 were used (Applied Biosystems). Mean normalized expression was calculated using the Q-Gene Application with GAPDH (Applied Biosystems) serving as endogenous control. At least three independent samples per group were analyzed. *Westerns*: Total protein was extracted from an equal number of cells in RIPA Lysis buffer with proteinase inhibitor cocktails. The lysates were then subjected to electrophoresis using NuPAGE Novex Gel system (Life Technologies) and were blotted to nitrocellulose membrane using iBlot Gel Transfer system (Life Technologies) according to manufacturer's instructions. Anti-IL3 antibody (AF-403-NA, R&D Systems) and anti-GAPDH (Ab9483, Abcam) antibody were used. *ELISA:* IL-1β, IL-3, IL-6, and TNF-α ELISA was performed with R&D ELISA kits according to the manufacturer's instructions on peritoneal lavage fluid, serum and cell culture supernatants. *Protein assay:* Total protein from the bronchoalveolar lavage (BAL) fluid was measured using the Bio-Rad Protein Assay according to the manufacturer's instructions. *AST and ALT*: AST and ALT were measured in plasma with Sigma kits according to the manufacturer's instructions.

Bacteria

Whole blood and peritoneal lavage samples were diluted, plated on tryptic soy agar (BD Difco), and incubated at 37ºC. The number of bacterial colonies was assessed 12-14 hours later. *Phagocytosis assay: PHrodo*™ labelled *Escherichia coli* particles (Invitrogen) were used following the manufacturer's instructions. Steady state peritoneal cells from control and *Il3*$^{-/-}$ mice were seeded at 3×10^5 cells/well in a 96 well plate.

Cells were allowed to seed 1 h at 37°C, the medium was then removed and replaced by medium with or without *E. coli* particles (1 mg/mL) and cells were incubated at 37°C or 4°C (negative control) for 2h. Cells were then retrieved and stained for flow cytometry. Phagocytosis rate was determined by the percentage of PHrodo/PE^{+} peritoneal macrophages.

Statistics

Human: For analysis of human data, wherever appropriate, data were visualized using line charts, bar charts or Kaplan-Meier plots. The Kolmogorov-Smirnov test was applied to check for normal distribution. Due to non-normally distributed data, non-parametric methods for evaluation were used (two-tailed non-parametric Wilcoxon matched pairs test or a two-tailed Mann Whitney U test). Multivariate logistic regression analyses were used to evaluate the input of IL-3 on the prediction of death at 28 days, and to adjust for potential confounders. *Mouse*: Results were expressed as identified in legends. For comparing 2 groups, statistical tests included unpaired, 2-tailed nonparametric Mann-Whitney tests (when Gaussian distribution was not assumed) or unpaired, 2-tailed parametric t tests with Welch's correction (when Gaussian distribution was assumed). For multiple comparisons, nonparametric multiple comparison's test (Kruskal-Wallis test with Dunn's multiple comparison) comparing mean rank of each group (when Gaussian distribution was not assumed) or 1-way ANOVA followed by Tukey's or Newman-Keuls Multiple Comparison Test were performed. P values of 0.05 or less were considered to denote significance.

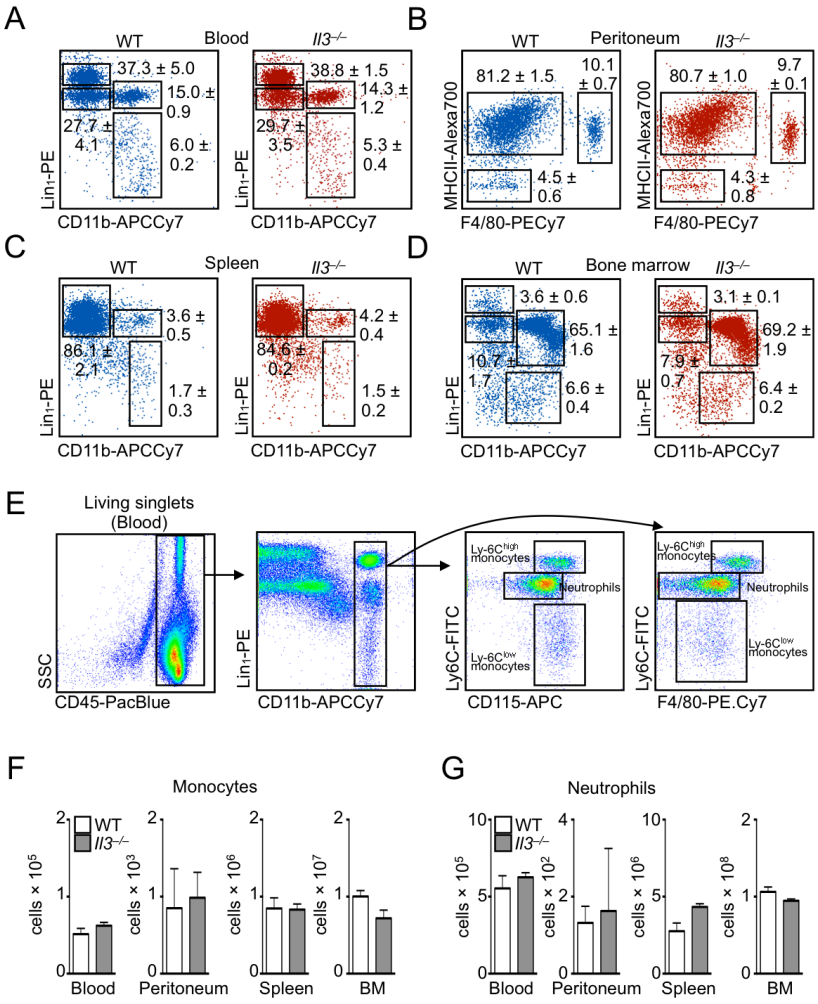

Fig. S1. Profiling Balb/c (WT) mice and *Il3*$^{-/-}$ mice in steady state and after CLP. Steady state analysis of (**A**) Blood. (**B**) Peritoneum. (**C**) Spleen. **(D)** Bone marrow. Representative dot plots of n > 5 are shown. (**E**) Gating strategy identifying monocytes and neutrophils in the blood. (**F**) Analysis of monocytes during steady state in blood, peritoneum, spleen and bone marrow. (**G**) Analysis of neutrophils during steady state in blood, peritoneum, spleen and bone marrow (n = 6 for all shown experiments). Error bars indicate means ± SEM.

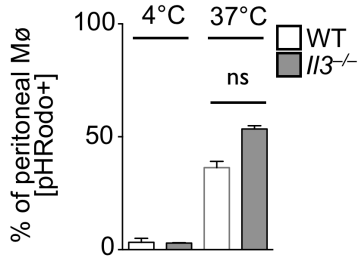

Fig. S2. IL-3 has no effect on phagocytosis. Phagocytic capacity in WT and *Il3*$^{-/-}$ cells in the steady state and 1 d after CLP (n = 3). Error bars indicate means ± SEM. Significance was assessed by Mann-Whitney test.

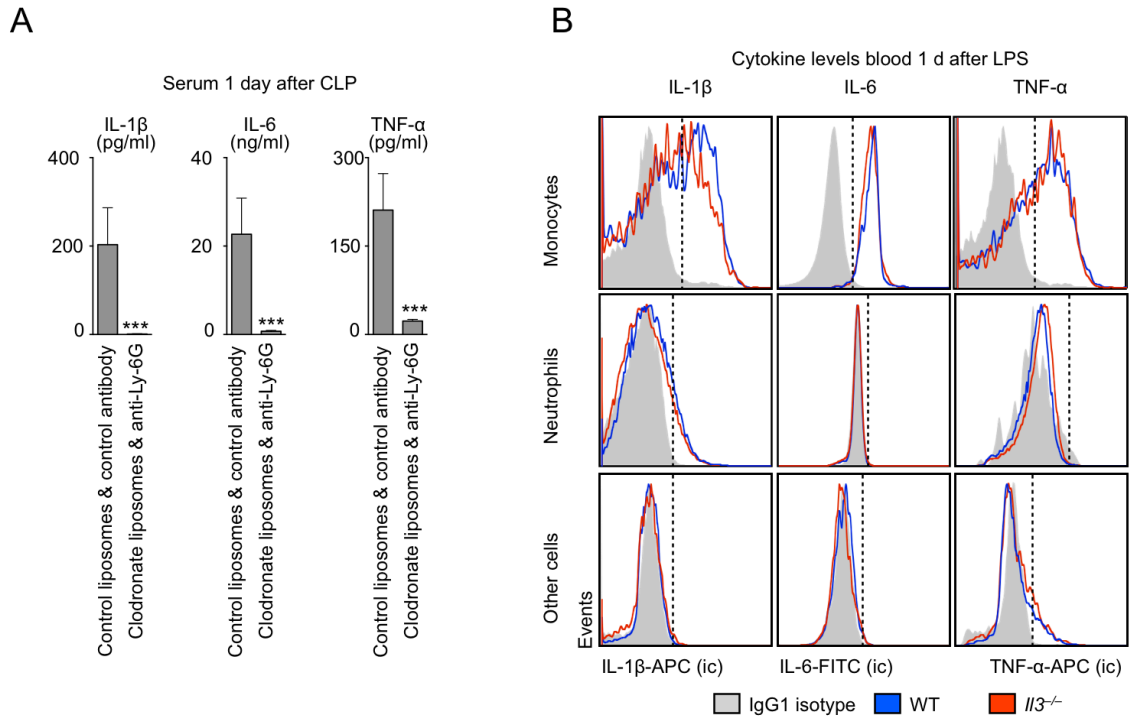

Fig. S3. IL-3 has no effects on myeloid production of inflammatory cytokines. (A) Serum IL-1β, IL-6 and TNF-α levels in WT mice 1 day after CLP. Mice received either control liposomes with isotype antibodies or clodronate liposomes with anti-Ly-6G antibodies prior to CLP (n=4; ***P<0.001). (**B**) Intracellular IL-1β, IL-6 and TNF-α staining gated on splenic monocytes, neutrophils, and other cells in WT and *Il3*$^{-/-}$ mice 1 day after LPS. The grey histogram denotes isotype staining. Error bars indicate means ± SEM. Significance was assessed by Mann-Whitney test (A).

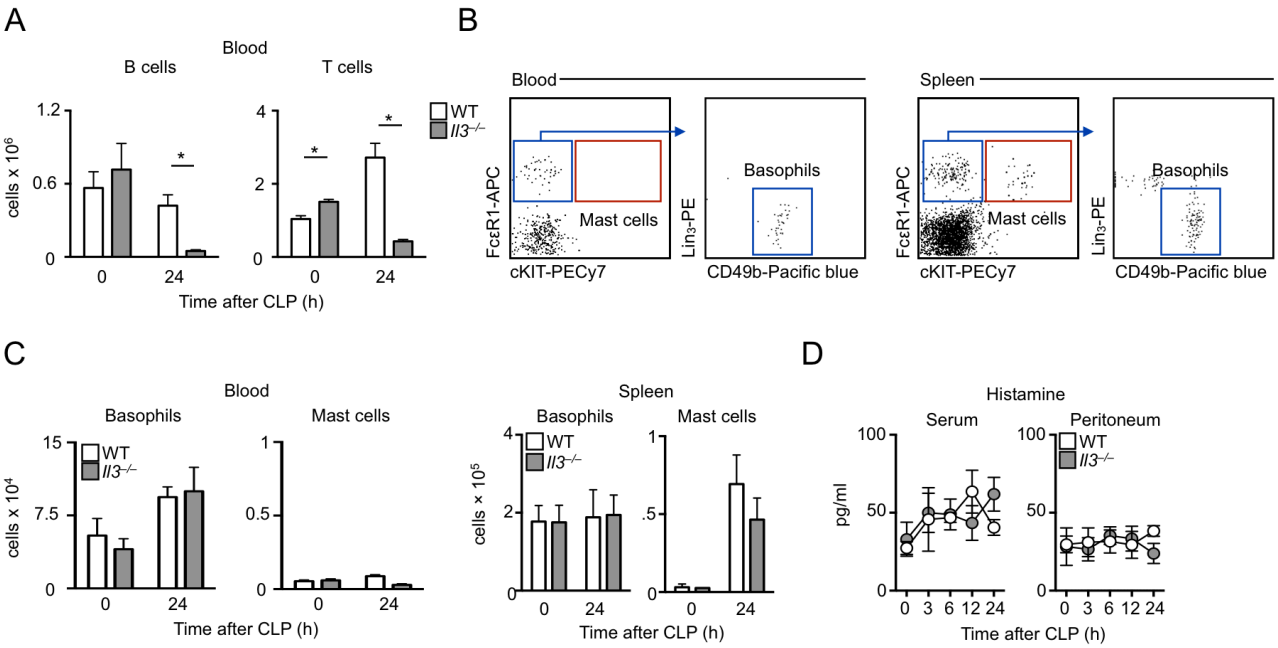

Fig. S4. Leukocyte flux after CLP. (**A**) Changes in T and B cell blood numbers in WT and *Il3*$^{-/-}$ mice 1 d after CLP (n=3). (**B**) Gating strategy for identifying basophils and mast cells. (**C**) Enumeration of basophils and mast cells in the blood and spleen at steady state and 1 d after CLP in WT and *Il3*$^{-/-}$ mice (means ± s.e.m.; n=3). (**D**) Histamine levels after CLP in the serum and peritoneum of WT and *Il3*$^{-/-}$ mice (n=3). Error bars indicate means ± SEM. Significance was assessed by Mann-Whitney test (A, C).

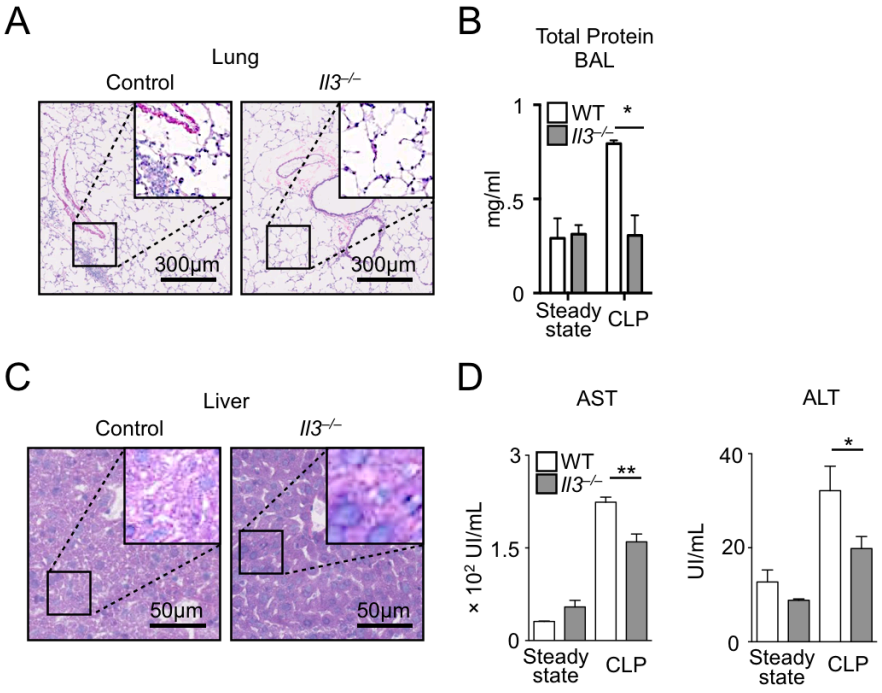

Fig. S5. IL-3 potentiates septic shock. (**A**) Hematoxylin and eosin (H&E) staining of lung sections 1 d after CLP (representative images of n = 5 are shown). (**B)** Measurement of total protein in the BAL 12 h post-CLP (n = 3). (**C**) H&E staining of liver sections 1 d after CLP (representative images of n = 5 are shown). **(D)** Aspartate aminotransferase (AST) and alanine aminotransferase (ALT) in the serum in the steady state and 1 d after CLP in the two groups (n = 3-5; *P<0.05, **P<0.01). Error bars indicate means ± SEM. Significance was assessed by Mann-Whitney test (B. D).

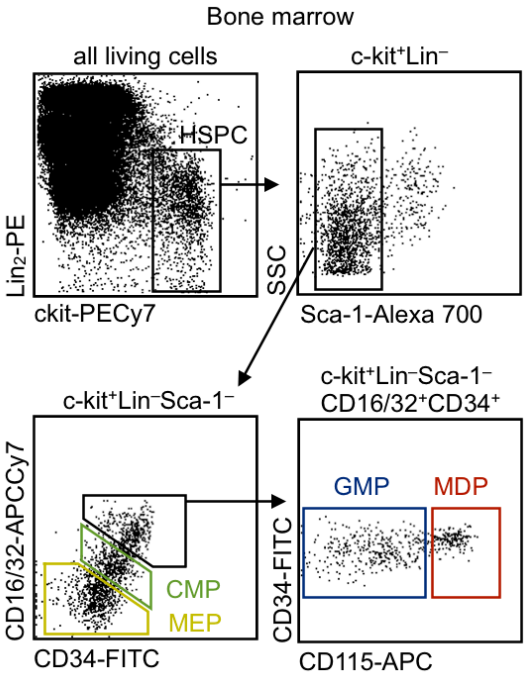

Fig. S6. HSPC gating strategy. Flow cytometry plots identifying Lin$^-$c-kit$^+$ hematopoietic stem and progenitor cells (HSPC), common myeloid progenitors (CMP), megakaryocyte and erythrocyte progenitors (MEP), granulocyte and macrophage progenitors (GMP), and macrophage and dendritic cell progenitors (MDP) in the bone marrow.

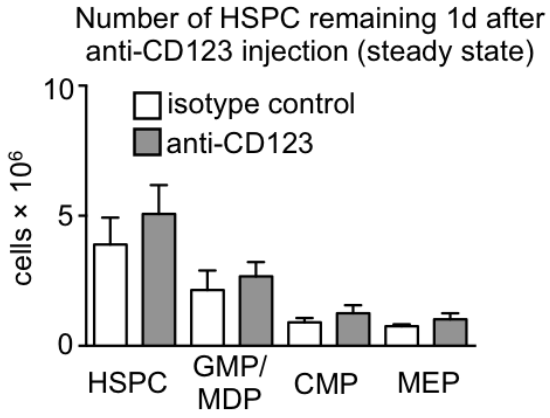

Fig. S7. Anti-CD123 antibody does not deplete HSPC. Enumeration of various HSPC in the bone marrow 1 d after injection of anti-CD123 or isotype to WT mice (n = 3; *P<0.05). Error bars indicate means ± SEM.

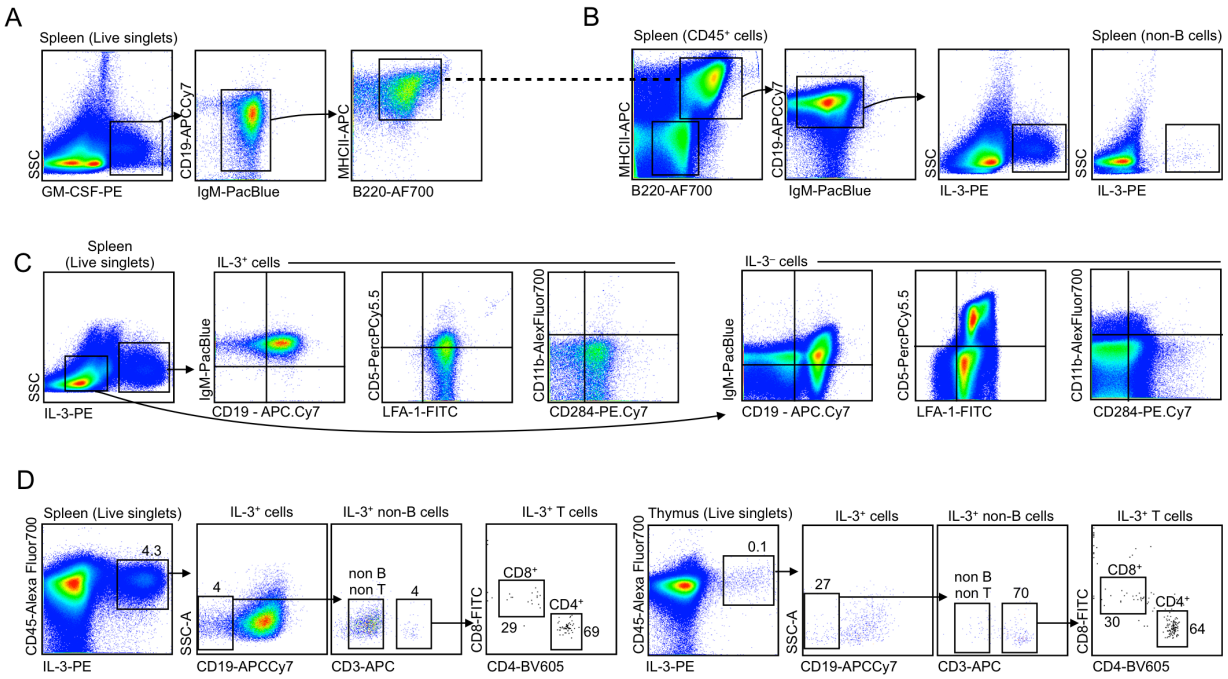

Fig. S8. IL-3-producing B cells are IRA B cells. (**A**) Identification of IRA B cells as GM-CSF-producing IgM$^+$ CD19$^+$ B220$^+$ MHCII$^+$ B cells. **(B)** IL-3-producing B cells are likewise IgM$^+$ CD19$^+$ B220$^+$ MHCII$^+$ B cells. Data were collected 4 d after CLP and representative plots of n = 4 are shown. **(C)** Detailed characterization of splenic IL-3-producing B cells as CD19$^+$ IgM$^+$ LFA-1^{int} CD5^{int} CD284$^+$ CD11b^{low}. Data were collected 4 d after CLP and representative plots of n = 4 are shown. **(D)** A minor population of IL-3 producing cells in the spleen and thymus consists of CD4$^+$ T cells, CD8$^+$ T cells, and non-T non-B cells. Representative plots of n = 4 are shown.

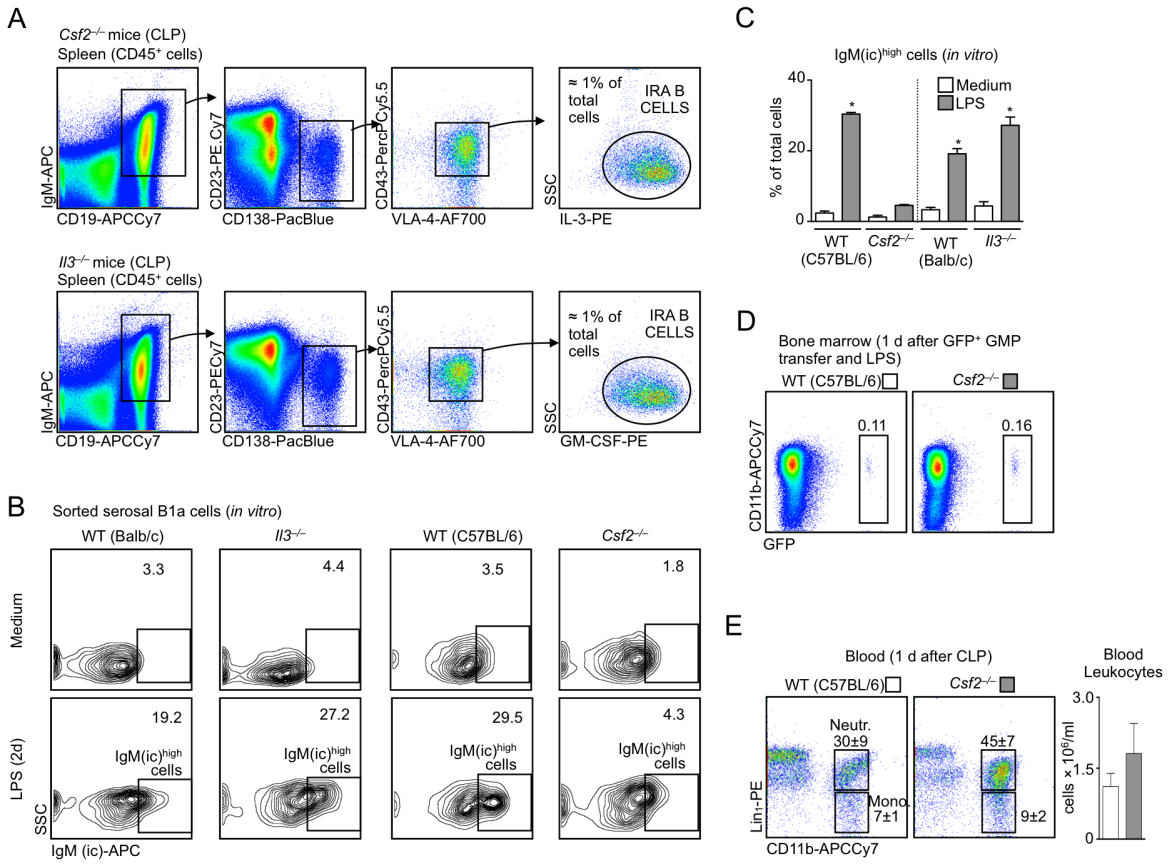

Fig. S9. IL-3 and GM-CSF produced by IRA B cells have distinct functions. (A) Identification of IL-3-producing IRA B cells in the spleen of GM-CSF-deficient (i.e., *Csf2*$^{-/-}$) mice 4 d after CLP and, conversely, identification of GM-CSF-producing IRA B cells in the spleen of IL-3-deficient (*Il3*$^{-/-}$) mice. Representative plots of n = 4 are shown. **(B)** Sorted B1a B cells from WT and *Il3*$^{-/-}$ mice were placed into culture and stimulated with LPS for 2 d. The cells were then stained to detect intracellular IgM levels. Data show that *Il3*$^{-/-}$ B1a cells augment intracelllar IgM levels at similar levels compared to WT cells. Cells producing IgM at high levels are termed IgM(ic)^{high}. **(C)** Enumeration of IgM(ic)^{high} cells produced after *in vitro* culture with LPS. Data show that GM-CSF is required for IgM(ic)^{high} cell production whereas IL-3 is dispensable (n = 3; *P<0.05). **(D)** GFP^{+} GMP sorted from the bone marrow of WT mice were adoptively transferred to either WT or *Csf2*$^{-/-}$ mice which then received LPS. 1 d after LPS, the bone marrow was analyzed. Data show GFP^{+} cells in recipients. The transferred cells differentiated to CD11b^{+} myeloid cells at similar frequencies. A representative of n = 3 plot is shown. **(E)** WT and *Csf2*$^{-/-}$ mice were subjected to CLP. Blood was analyzed 1 d later. Data show heightened neutrophil concentrations and an overall higher trend in leukocyte number in the *Csf2*$^{-/-}$ mice indicating GM-CSF is dispensable for myelopoiesis in response to CLP (n = 3). Error bars indicate means ± SEM. Significance was assessed by t test.

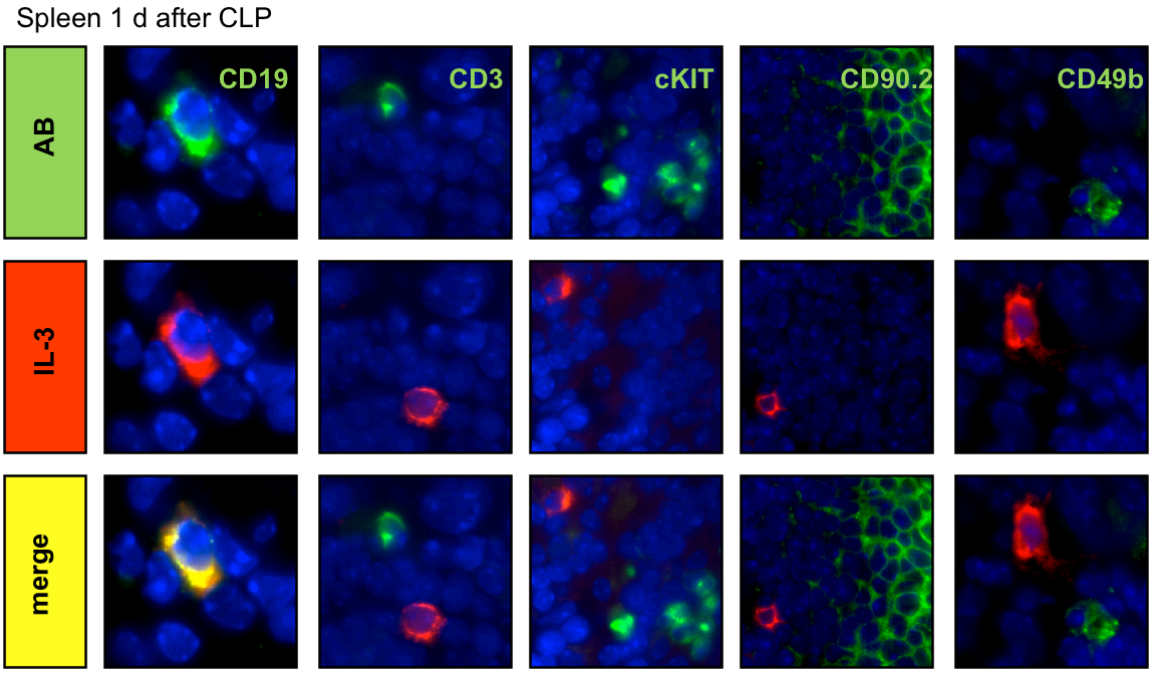

Fig. S10. Characterization of IL-3 producing cells after CLP. Immunofluorescence microscopy in the splenic red pulp identifies IL-3$^+$ B cells as CD19$^+$ and CD3$^-$ c-kit$^-$ CD90.2$^-$ CD49b$^-$. Representatives of >100 cells examined are shown.

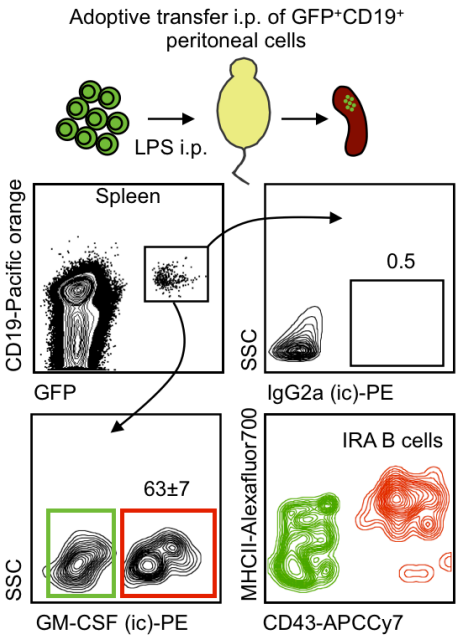

Fig. S11. Adoptive transfer of peritoneal B1a B cells yields GM-CSF$^+$ cells. Cells from steady state GFP$^+$ mice were transferred to WT mice that then received LPS for 2 days. Animals were analyzed 48 h after transfer. Representative plots from flow cytometric analysis of n = 3 are shown.

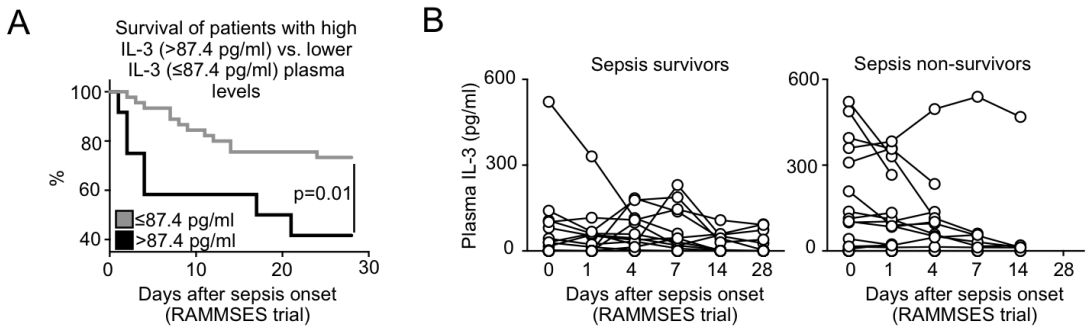

Fig. S12. Association of IL-3 plasma levels with survival in the RAMMSES cohort. (**A)** Kaplan-Meier analysis showing survival of patients in the RAMMSES cohort with IL-3 at >87.4 pg/ml (top quintile, measured 1 day after sepsis onset) vs. patients with IL-3 ≤ 87.4 pg/ml. (**B**) IL-3 plasma levels in patients with sepsis over 28 d after sepsis onset. Data show levels in sepsis survivors and sepsis non-survivors in the RAMMSES study. Significance was assessed by logrank (A).

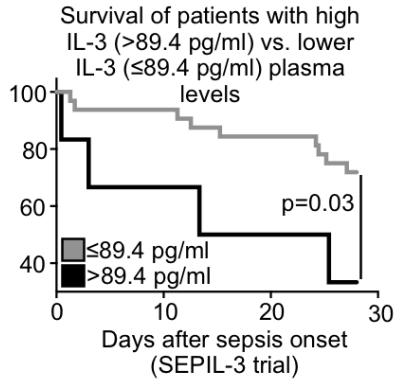

Fig. S13. Association of IL-3 plasma levels with survival in the SEPIL-3 cohort. Kaplan-Meier analysis showing survival of patients in the SEPIL-3 cohort with IL-3 at >89.4 pg/ml (top quintile, measured within 1 day after sepsis onset) vs. patients with IL-3 ≤ 87.4 pg/ml.

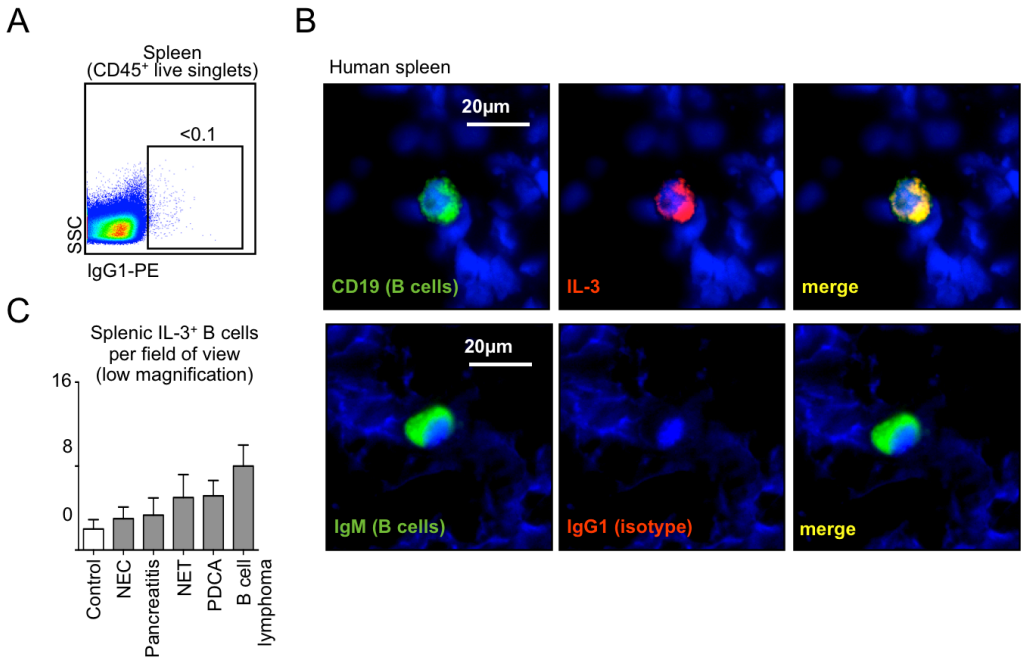

Fig. S14. B cells are sources of IL-3 in the human spleen. (**A**) Flow cytometry plot showing IgG1-PE isotype control in human splenocytes. (**B**) Immunofluorescence of human spleen showing co-staining of IgM-FITC, CD19-FITC, IL-3-PE, and IgG1-PE isotype control. One representative slide from n = 6 is shown. (**C**) Enumeration of IL-3 producing B cells in 6 different patients. (NET/C=neuroendocrine tumor/cancer of the pancreas; PDCA=pancreatic ductal cancer). Error bars indicate means ± SEM.

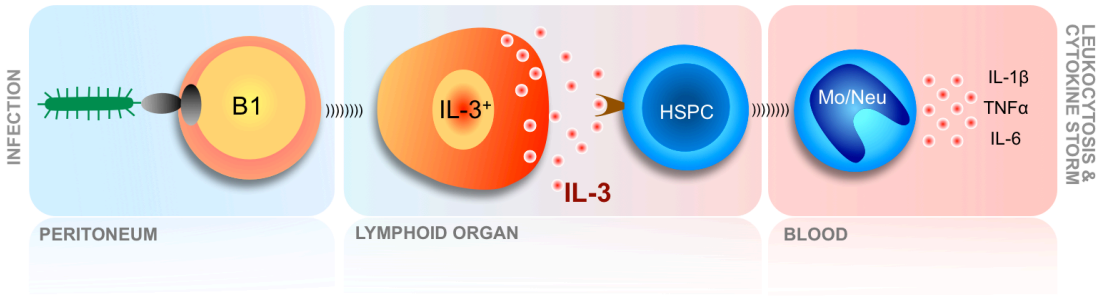

Fig. S15. Model. Peritoneal B1a cells are activated by microbial pathogens and give rise to IL-3^{+} B cells in the red pulp of the spleen. IL-3 acts on HSPC to promote the emergency generation of inflammatory leukocytes that are released into the circulation. This leads to an uncontrolled cytokine storm, multi-organ failure, septic shock, and death.

Table S1. Patients' characteristics (*RAMMSES-trial*).

Table S2: Patients' characteristics separated by IL-3 levels (*RAMMSES-trial*).

RAMMSES-trial - Patients with septic shock (n=60)	
Demographic data	
Age (y)	68.6 ±11.7
Male sex	46 (76.7%)
ASA-Status: I; II; III; IV; V	1(1.7%); 11(18.3%); 29(48.3%); 15(25.0%); 1(1.7%)
Sites of infection	
Gastrointestinal tract	32 (53.3%)
Surgical site	16 (26.7%)
Genitourinary tract	6 (10.0%)
Pulmonary site	12 (20.0%)
Others	2 (3.3%)
Septic organ failure	
ARF	35 (58.3%)
ARDS	49 (81.2%)
ALF	15 (25.0%)
Outcome	
Survivor 28d	38 (63.3%)
Disease Severity Scoring	
APACHE II	32 ± 19
SAPS	74 ± 18
SOFA	13 ± 3
Laboratory parameters	
Leukocyte count [1/nl]	16 ± 10
C-reactive protein [mg/l]	161 ± 51
Procalcitonine [µg/l]	17 ± 31
Lactate [mg/dl]	33 ± 34
Clinical data	
Norepinephrine [µg/kg/min]	0.21± 0.18
Max. HR [1/min]	115 ± 22
Min. MAP [mmHg]	58 ± 11
FiO2 [none]	0.67 ± 0.19
PaO2 [mmHg]	n.a.
BMI [kg/m^2]	n.a.
Max. body temperature [ºC]	37.0 ± 1.0

Data presented by number (%) or by mean ± standard deviation.

Abbreviations: ASA, American Society of Anesthesiologists; ARF, acute renal failure; ARDS, acute respiratory distress syndrome; ALF, acute liver failure; APACHE II, acute physiology and chronic health evaluation II; SAPS, simplified acute physiology score; SOFA, sequential organ failure assessment; HR, heart rate; MAP; middle arteriel pressure; min, minimal; max, maximal; FiO2, fraction of inspired oxygen; PaO2, partial oxygen pressure; BMI, body mass index

Table S3. Patients' characteristics (*SEPIL-3-trial*).

RAMMSES-trial - Patients with septic shock at day 1 (n=56)			
	IL-3>87.4pg/ml (n=12)	**IL-3≤87.4pg/ml (n=44)**	**p-value**
Demographic data			
Age (y)	71.1±8.0	66.9±12.0	0.453
Male sex	8 (66.7%)	36 (81.8%)	0.257
ASA-Status			
ASA I	0 (0.0%)	1 (2.3%)	0.590
ASA II	4 (33.3%)	7 (15.9%)	0.206
ASA III	2 (16.7%)	23 (52.3%)	**0.020***
ASA IV	6 (50.0%)	9 (20.5%)	0.051
ASA V	0 (0.0%)	1 (2.3%)	0.590
Sites of infection			
Gastrointestinal tract	8 (66.7%)	22 (50.0%)	0.424
Genitourinary tract	3 (25.0%)	2 (4.5%)	**0.036***
Pulmonary site	1 (8.3%)	11 (25.0%)	0.178
Surgical site	5 (41.7%)	10 (22.7%)	0.243
Others	1 (8.3%)	1 (2.3%)	0.357
Septic organ failure			
ARF	8 (66.7%)	25 (56.8%)	0.594
ARDS	11 (91.7%)	36 (81.8%)	0.710
ALF	5 (41.7%)	10 (22.7%)	0.189
Outcome			
Survivor 28d	5 (41.7%)	35 (79.5%)	**0.010***
Disease Severity Scoring			
APACHE II	31±7	33±9	0.309
SAPS	77±13	73±19	0.512
SOFA	14±3	13±3	0.276
Laboratory parameters			
Leukocyte count [1/nl]	17±8	16±11	0.523
C-reactive protein [mg/l]	140±41	171±50	**0.027***
Procalcitonine [µg/l]	13±19	19±35	0.750
Lactate [mg/dl]	37±31	29±32	0.213
Clinical data			
Norepinephrine [µg/kg/min]	0.26±0.18	0.19±0.16	0.169
Max. HR [1/min]	112±21	117±22	0.361
Min. MAP [mmHg]	57±10	58±12	0.868
FiO2 [none]	0.64±0.22	0.67±0.19	0.387
PaO2 [mmHg]	n.a.	n.a.	n.a.
BMI [kg/m^2]	n.a.	n.a.	n.a.
Max. body temperature [°C]	36.6±1.4	37.2±0.9	0.117
Data presented by number (%) or by mean ± standard deviation.			

Table S4. Patients' characteristics separated by IL-3 levels (*SEPIL-3-trial*).

SEPIL-3-trial - Patients with septic shock (n=37)	
Demographic data	
Age (y)	65.8 ± 13.6
Male sex	37 (92.5%)
ASA-Status: I; II; III; IV; V	0(0%); 2(5%); 8(20%); 28(70%); 2(5%)
Sites of infection	
Gastrointestinal tract	29 (72.5%)
Surgical site	n.a.
Genitourinary tract	4 (10.0%)
Pulmonary site	12 (30.0%)
Others	5 (12.5%)
Septic organ failure	
ARF	9 (22.5%)
ARDS	14 (35.0%)
ALF	13 (32.5%)
Outcome	
Survivor 28d	25 (62.5%)
Disease Severity Scoring	
APACHE II	n.a.
SAPS	n.a.
SOFA	12 ± 4
Laboratory parameters	
Leukocyte count [1/nl]	17 ± 9
C-reactive protein [mg/l]	210 ± 109
Procalcitonine [µg/l]	19 ± 38
Lactate [mg/dl]	45 ± 38
Clinical data	
Norepinephrine [µg/kg/min]	0.22 ± 0.19
Max. HR [1/min]	n.a.
Min. MAP [mmHg]	64 ± 11
FiO2 [none]	0.53 ± 0.22
PaO2 [mmHg]	75 ± 15
BMI [kg/m^2]	28.3 ± 11.6
Max. body temperature [ºC]	n.a.

Data presented by number (%) or by mean ± standard deviation.

Abbreviations: ASA, American Society of Anesthesiologists; ARF, acute renal failure; ARDS, acute respiratory distress syndrome; ALF, acute liver failure; APACHE II, acute physiology and chronic health evaluation II; SAPS, simplified acute physiology score; SOFA, sequential organ failure assessment; HR, heart rate; MAP; middle arteriel pressure; min, minimal; max, maximal; FiO2, fraction of inspired oxygen; partial oxygen pressure; BMI, body mass index

Table S5. Multivariate logistic regression analyses of parameters associated with 28 d

SEPIL-3-trial - Patients with septic shock at sepsis onset (n=37)			
	IL-3>89.4pg/ml (n=6)	**IL-3≤89.4pg/ml (n=31)**	**p-value**
Demographic data			
Age (y)	67.3±12.2	63.9±14.3	0.582
Male sex	6 (100.0%)	28 (90.3%)	0.441
ASA-Status			
ASA I	0 (0.0%)	0 (0.0%)	ø
ASA II	0 (0.0%)	2 (6.5%)	0.161
ASA III	0 (0.0%)	7 (22.6%)	**0.006****
ASA IV	5 (83.3%)	22 (71.0%)	0.526
ASA V	1 (16.7%)	0 (0.0%)	0.363
Sites of infection			
Gastrointestinal tract	4 (66.7%)	25 (80.7%)	0.460
Genitourinary tract	0 (0.0%)	4 (12.9%)	0.365
Pulmonary site	3 (50.0%)	8 (25.8%)	0.247
Surgical site	n.a.	n.a.	n.a.
Others	1 (16.7%)	4 (12.9%)	0.812
Septic organ failure			
ARF	2 (33.3%)	6 (19.4%)	0.460
ARDS	3 (50.0%)	10 (32.3%)	0.419
ALF	1 (16.7%)	11 (35.5%)	0.382
Outcome			
Survivor 28d	2 (33.3%)	22 (71.0%)	**0.031***
Disease Severity Scoring			
APACHE II	n.a.	n.a.	n.a.
SAPS	n.a.	n.a.	n.a.
SOFA	12±2	11±4	0.500
Laboratory parameters			
Leukocyte count [1/nl]	17±10	16±11	0.826
C-reactive protein [mg/l]	183±103	246±92	0.167
Procalcitonine [µg/l]	23±28	22±27	0.980
Lactate [mg/dl]	80±56	40±33	**0.020***
Clinical data			
Norepinephrine [µg/kg/min]	0.28±0.18	0.21±0.20	0.419
Max. HR [1/min]	n.a.	n.a.	n.a.
Min. MAP [mmHg]	63±7	64±14	0.899
FiO2 [none]	0.59±0.22	0.53±0.23	0.572
PaO2 [mmHg]	76±14	75±15	0.807
BMI [kg/m^2]	29.3±1.1	28.1±12.0	0.730
Max. body temperature [ºC]	n.a.	n.a.	n.a.
Data presented by number (%) or by mean ± standard deviation.			

mortality (*RAMMSES and SEPIL-3 cohorts*).

	model p-value	p-values associated with IL-3	OR association with IL-3 (95% CI)
IL-3 + ARF + age + cohort	0.019	0.006	4.9 [1.6-15.3]
IL-3 + ALF + age + cohort	0.04	0.004	5.1 [1.7-15.4]
IL-3 + age + cohort	0.022	0.004	5.1 [1.7-15.6]
IL-3 + ASA + age + cohort	0.002	0.041	3.8 [1.1-13.5]
IL-3 + gender + age + cohort	0.042	0.004	5.3 [1.7-16.3]
IL-3 + lactate + age + cohort	0.023	0.023	3.8 [1.2-12]
IL-3 + norepinephrine + age + cohort	0.034	0.004	5.2 [1.7-15.9]
IL-3 + SOFA + age + cohort	0.039	0.018	4 [1.3-12.3]
IL-3 + APACHE + age*	0.089	0.05	4.6 [1-21.8]
IL-3 + SAPS + age*	0.016	0.03	5.4 [1.1-25.8]

*performed only on the RAMMSES cohort. The effect of the center was measured as an independent variable (<<cohort>>) and added to each model.
OR: Odds Ratio
CI: Confidence interval

Table S6. Evolution of the pseudo-R-Squared (pseudo-R^2) and Aikake Information Criterion (AIC) values (*RAMMSES and SEPIL-3 cohorts*).

	AIC		Pseudo-R2	
	Without IL-3	**With IL-3**	**WIthout IL-3**	**WIth IL-3**
ARF + age + cohort	128	113	0.03	0.10
ALF + age + cohort	129	115	0.01	0.09
age + cohort	129	114	0.01	0.08
ASA + age + cohort	120	107	0.13	0.20
gender + age + cohort	131	115	0.01	0.09
lactate + age + cohort	116	110	0.03	0.09
norepinephrine + age + cohort	115	109	0.02	0.10
SOFA + age + cohort	114	110	0.04	0.09
APACHE + age*	63	61	0.05	0.11
SAPS + age*	63	60	0.09	0.17

*performed only on the RAMMSES cohort. The effect of the center was measured as an independent variable (<<cohort>>) and added to each model.
AIC: Aikake Information Criteria.

REFERENCES AND NOTES

1. Y. C. Yang, A. B. Ciarletta, P. A. Temple, M. P. Chung, S. Kovacic, J. A. S. Witek-Giannotti, A. C. Leary, R. Kriz, R. E. Donahue, G. G. Wong, S. C. Clark, Human IL-3 (multi-CSF): Identification by expression cloning of a novel hematopoietic growth factor related to murine IL-3. *Cell* **47**, 3–10 (1986). Medline doi:10.1016/0092-8674(86)90360-0

2. A. J. Hapel, J. C. Lee, W. L. Farrar, J. N. Ihle, Establishment of continuous cultures of thy1.2+, Lyt1+, 2-T cells with purified interleukin 3. *Cell* **25**, 179–186 (1981). Medline doi:10.1016/0092-8674(81)90242-7

3. J. N. Ihle, L. Pepersack, L. Rebar, Regulation of T cell differentiation: In vitro induction of 20 alpha-hydroxysteroid dehydrogenase in splenic lymphocytes from athymic mice by a unique lymphokine. *J. Immunol.* **126**, 2184–2189 (1981). Medline

4. G. T. Williams, C. A. Smith, E. Spooncer, T. M. Dexter, D. R. Taylor, Haemopoietic colony stimulating factors promote cell survival by suppressing apoptosis. *Nature* **343**, 76–79 (1990). Medline doi:10.1038/343076a0

5. D. C. Angus, T. van der Poll, Severe sepsis and septic shock. *N. Engl. J. Med.* **369**, 840–851 (2013). Medline doi:10.1056/NEJMra1208623

6. R. S. Hotchkiss, G. Monneret, D. Payen, Sepsis-induced immunosuppression: From cellular dysfunctions to immunotherapy. *Nat. Rev. Immunol.* **13**, 862–874 (2013). Medline doi:10.1038/nri3552

7. C. S. Deutschman, K. J. Tracey, Sepsis: Current dogma and new perspectives. *Immunity* **40**, 463–475 (2014). Medline doi:10.1016/j.immuni.2014.04.001

8. Materials and methods are available as supplementary materials on *Science* Online.

9. D. Rittirsch, M. S. Huber-Lang, M. A. Flierl, P. A. Ward, Immunodesign of experimental sepsis by cecal ligation and puncture. *Nat. Protoc.* **4**, 31–36 (2009). Medline doi:10.1038/nprot.2008.214

10. M. C. Jamur, C. Oliver, Origin, maturation and recruitment of mast cell precursors. *Front. Biosci. (Schol. Ed.)* **S3**, 1390–1406 (2011). Medline doi:10.2741/231

11. D. Voehringer, Basophil modulation by cytokine instruction. *Eur. J. Immunol.* **42**, 2544–2550 (2012). Medline doi:10.1002/eji.201142318

12. E. Rönnberg, C. F. Johnzon, G. Calounova, G. Garcia Faroldi, M. Grujic, K. Hartmann, A. Roers, B. Guss, A. Lundequist, G. Pejler, Mast cells are activated by *Staphylococcus aureus* in vitro but do not influence the outcome of intraperitoneal *S. aureus* infection in vivo. *Immunology* **143**, 155–163 (2014). Medline doi:10.1111/imm.12297

13. D. Annane, E. Bellissant, J. M. Cavaillon, Septic shock. *Lancet* **365**, 63–78 (2005). Medline doi:10.1016/S0140-6736(04)17667-8

14. P. A. Ward, New approaches to the study of sepsis. *EMBO Mol. Med.* **4**, 1234–1243 (2012). Medline doi:10.1002/emmm.201201375

15. M. Kondo, A. J. Wagers, M. G. Manz, S. S. Prohaska, D. C. Scherer, G. F. Beilhack, J. A. Shizuru, I. L. Weissman, Biology of hematopoietic stem cells and progenitors:

Implications for clinical application. *Annu. Rev. Immunol.* **21**, 759–806 (2003). Medline doi:10.1146/annurev.immunol.21.120601.141007

16. J. E. Groopman, J. M. Molina, D. T. Scadden, Hematopoietic growth factors. Biology and clinical applications. *N. Engl. J. Med.* **321**, 1449–1459 (1989). Medline doi:10.1056/NEJM198911233212106

17. A. H. Dalloul, M. Arock, C. Fourcade, A. Hatzfeld, J. M. Bertho, P. Debré, M. D. Mossalayi, Human thymic epithelial cells produce interleukin-3. *Blood* **77**, 69–74 (1991). Medline

18. P. J. Rauch, A. Chudnovskiy, C. S. Robbins, G. F. Weber, M. Etzrodt, I. Hilgendorf, E. Tiglao, J. L. Figueiredo, Y. Iwamoto, I. Theurl, R. Gorbatov, M. T. Waring, A. T. Chicoine, M. Mouded, M. J. Pittet, M. Nahrendorf, R. Weissleder, F. K. Swirski, Innate response activator B cells protect against microbial sepsis. *Science* **335**, 597–601 (2012). Medline doi:10.1126/science.1215173

19. G. F. Weber, B. G. Chousterman, I. Hilgendorf, C. S. Robbins, I. Theurl, L. M. Gerhardt, Y. Iwamoto, T. D. Quach, M. Ali, J. W. Chen, T. L. Rothstein, M. Nahrendorf, R. Weissleder, F. K. Swirski, Pleural innate response activator B cells protect against pneumonia via a GM-CSF-IgM axis. *J. Exp. Med.* **211**, 1243–1256 (2014). Medline doi:10.1084/jem.20131471

20. I. Hilgendorf, I. Theurl, L. M. Gerhardt, C. S. Robbins, G. F. Weber, A. Gonen, Y. Iwamoto, N. Degousee, T. A. Holderried, C. Winter, A. Zirlik, H. Y. Lin, G. K. Sukhova, J. Butany, B. B. Rubin, J. L. Witztum, P. Libby, M. Nahrendorf, R. Weissleder, F. K. Swirski, Innate response activator B cells aggravate atherosclerosis by stimulating T helper-1 adaptive immunity. *Circulation* **129**, 1677–1687 (2014). Medline doi:10.1161/CIRCULATIONAHA.113.006381

21. S. A. Ha, M. Tsuji, K. Suzuki, B. Meek, N. Yasuda, T. Kaisho, S. Fagarasan, Regulation of B1 cell migration by signals through Toll-like receptors. *J. Exp. Med.* **203**, 2541–2550 (2006). Medline doi:10.1084/jem.20061041

22. J. Seok, H. S. Warren, A. G. Cuenca, M. N. Mindrinos, H. V. Baker, W. Xu, D. R. Richards, G. P. McDonald-Smith, H. Gao, L. Hennessy, C. C. Finnerty, C. M. López, S. Honari, E. E. Moore, J. P. Minei, J. Cuschieri, P. E. Bankey, J. L. Johnson, J. Sperry, A. B. Nathens, T. R. Billiar, M. A. West, M. G. Jeschke, M. B. Klein, R. L. Gamelli, N. S. Gibran, B. H. Brownstein, C. Miller-Graziano, S. E. Calvano, P. H. Mason, J. P. Cobb, L. G. Rahme, S. F. Lowry, R. V. Maier, L. L. Moldawer, D. N. Herndon, R. W. Davis, W. Xiao, R. G. Tompkins, A. Abouhamze, U. G. J. Balis, D. G. Camp, A. K. De, B. G. Harbrecht, D. L. Hayden, A. Kaushal, G. E. O'Keefe, K. T. Kotz, W. Qian, D. A. Schoenfeld, M. B. Shapiro, G. M. Silver, R. D. Smith, J. D. Storey, R. Tibshirani, M. Toner, J. Wilhelmy, B. Wispelwey, W. H. Wong; Inflammation and Host Response to Injury, Large Scale Collaborative Research Program, Genomic responses in mouse models poorly mimic human inflammatory diseases. *Proc. Natl. Acad. Sci. U.S.A.* **110**, 3507–3512 (2013). Medline doi:10.1073/pnas.1222878110

23. K. Takao, T. Miyakawa, Genomic responses in mouse models greatly mimic human inflammatory diseases. *Proc. Natl. Acad. Sci. U.S.A.* **112**, 1167–1172 (2015). Medline

24. T. Brenner, T. Fleming, F. Uhle, S. Silaff, F. Schmitt, E. Salgado, A. Ulrich, S. Zimmermann, T. Bruckner, E. Martin, A. Bierhaus, P. P. Nawroth, M. A. Weigand, S.

Hofer, Methylglyoxal as a new biomarker in patients with septic shock: An observational clinical study. *Crit. Care* **18**, 683 (2014). Medline doi:10.1186/s13054-014-0683-x

25. G. S. Martin, D. M. Mannino, S. Eaton, M. Moss, The epidemiology of sepsis in the United States from 1979 through 2000. *N. Engl. J. Med.* **348**, 1546–1554 (2003). Medline doi:10.1056/NEJMoa022139

26. K. A. Wood, D. C. Angus, Pharmacoeconomic implications of new therapies in sepsis. *Pharmacoeconomics* **22**, 895–906 (2004). Medline doi:10.2165/00019053-200422140-00001

27. M. Bosmann, P. A. Ward, The inflammatory response in sepsis. *Trends Immunol.* **34**, 129–136 (2013). Medline doi:10.1016/j.it.2012.09.004

28. C. M. Coopersmith, H. Wunsch, M. P. Fink, W. T. Linde-Zwirble, K. M. Olsen, M. S. Sommers, K. J. Anand, K. M. Tchorz, D. C. Angus, C. S. Deutschman, A comparison of critical care research funding and the financial burden of critical illness in the United States. *Crit. Care Med.* **40**, 1072–1079 (2012). Medline doi:10.1097/CCM.0b013e31823c8d03

29. E. Dolgin, Trial failure prompts soul-searching for critical-care specialists. *Nat. Med.* **18**, 1000 (2012). Medline doi:10.1038/nm0712-1000

30. S. M. Opal, C. J. Fisher Jr., J. F. Dhainaut, J. L. Vincent, R. Brase, S. F. Lowry, J. C. Sadoff, G. J. Slotman, H. Levy, R. A. Balk, M. P. Shelly, J. P. Pribble, J. F. LaBrecque, J. Lookabaugh, H. Donovan, H. Dubin, R. Baughman, J. Norman, E. DeMaria, K. Matzel, E. Abraham, M. Seneff, Confirmatory interleukin-1 receptor antagonist trial in severe sepsis: A phase III, randomized, double-blind, placebo-controlled, multicenter trial. The Interleukin-1 Receptor Antagonist Sepsis Investigator Group. *Crit. Care Med.* **25**, 1115–1124 (1997). Medline doi:10.1097/00003246-199707000-00010

31. J. S. Boomer, K. To, K. C. Chang, O. Takasu, D. F. Osborne, A. H. Walton, T. L. Bricker, S. D. Jarman 2nd, D. Kreisel, A. S. Krupnick, A. Srivastava, P. E. Swanson, J. M. Green, R. S. Hotchkiss, Immunosuppression in patients who die of sepsis and multiple organ failure. *JAMA* **306**, 2594–2605 (2011). Medline doi:10.1001/jama.2011.1829

32. R. S. Hotchkiss, C. M. Coopersmith, J. E. McDunn, T. A. Ferguson, The sepsis seesaw: Tilting toward immunosuppression. *Nat. Med.* **15**, 496–497 (2009). Medline doi:10.1038/nm0509-496

33. P. A. Ward, Immunosuppression in sepsis. *JAMA* **306**, 2618–2619 (2011). Medline doi:10.1001/jama.2011.1831

34. M. M. Levy, M. P. Fink, J. C. Marshall, E. Abraham, D. Angus, D. Cook, J. Cohen, S. M. Opal, J. L. Vincent, G. Ramsay; SCCM/ESICM/ACCP/ATS/SIS, 2001 SCCM/ESICM/ACCP/ATS/SIS International Sepsis Definitions Conference. *Crit. Care Med.* **31**, 1250–1256 (2003). Medline doi:10.1097/01.CCM.0000050454.01978.3B

35. K. Ohmori, Y. Luo, Y. Jia, J. Nishida, Z. Wang, K. D. Bunting, D. Wang, H. Huang, IL-3 induces basophil expansion in vivo by directing granulocyte-monocyte progenitors to differentiate into basophil lineage-restricted progenitors in the bone marrow and by increasing the number of basophil/mast cell progenitors in the spleen. *J. Immunol.* **182**, 2835–2841 (2009). Medline doi:10.4049/jimmunol.0802870

36. G. A. Colvin, J. F. Lambert, M. Abedi, C. C. Hsieh, J. E. Carlson, F. M. Stewart, P. J. Quesenberry, Murine marrow cellularity and the concept of stem cell competition: Geographic and quantitative determinants in stem cell biology. *Leukemia* **18**, 575–583 (2004). Medline doi:10.1038/sj.leu.2403268